https://doi.org/10.5194/egusphere-2024-3195
Preprint. Discussion started: 18 October 2024

Explaining the period fluctuation of the quasi-biennial oscillation

Young-Ha Kim[1]

[1]Research Institute of Basic Sciences, Seoul National University, Seoul, Republic of Korea

Correspondence: Young-Ha Kim (kyha0830@snu.ac.kr)

Abstract. The tropical stratosphere is characterized by a periodic oscillation of wind direction between westerly and easterly, known as the quasi-biennial oscillation, which modulates middle atmospheric circulations and surface climate on interannual time scales. The oscillation period fluctuates irregularly between 20 and 35 months. The causes of this fluctuation have long been hypothesized but lack observational evidence. This study shows that the period fluctuation is primarily driven by variability in small-scale wave (gravity wave) activity. Using an atmospheric reanalysis dataset, we capture temporal variations in small-scale wave activity that are coherent with the varying speed of the oscillation. This wave activity variation stems from the seasonality of tropical convection and tropopause-layer wind, revealing their fundamental role in modulating the quasi-biennial period. Our findings suggest that better representing these multi-scale interactions in models can enhance the accuracy of seasonal forecasts and the reliability of future climate projections.

1 Introduction

The wind in the tropical stratosphere alternates between an easterly and westerly direction with periods varying irregularly from 20 to 35 months (Baldwin et al., 2001; Anstey et al., 2022a). This so-called quasi-biennial oscillation (QBO) is intense enough in amplitude ($\sim$30 $\mathrm{m\,s^{-1}}$) to modulate the extratropical circulation and global distributions of chemical species (e.g., Holton and Tan, 1980; Ling and London, 1986; Randel and Wu, 1996; Kinnersley and Tung, 1998; Flury et al., 2013). The alternating wind phases propagate down to the tropopause layer ($\sim$18 km altitude). Recent studies have revealed further downward impacts of the QBO on surface weather and climate in the tropics (Haynes et al., 2021; Yoo and Son, 2016) and extratropics through atmospheric teleconnections (Thompson et al., 2002; Garfinkel and Hartmann, 2011; Gray et al., 2018; Anstey et al., 2022b). The QBO is therefore regarded as an important climate mode that can enhance the skill of seasonal and decadal predictions, provided that it is reproduced well by forecasting models (Scaife et al., 2014; Coy et al., 2022).

A barrier to the successful prediction of the QBO is the variability in its period and phase progression. The speed of phase progression varies, largely depending on the calendar month, and accordingly, the lengths of individual oscillation cycles fluctuate (e.g., Dunkerton, 1990; Wallace et al., 1993; Schenzinger et al., 2017; Coy et al., 2020). Current seasonal prediction models are deficient in capturing the varying timings of phase transition, which limits the forecast skill of the oscillation beyond the lead time of a few months (Stockdale et al., 2022; Coy et al., 2022). In line with this, climate models tend to reveal a lack of variability in the QBO period in multi-decadal simulations (Bushell et al., 2022). Regarding this problem, a fundamental

https://doi.org/10.5194/egusphere-2024-3195
Preprint. Discussion started: 18 October 2024

question is the underlying process driving the observed fluctuations in the period and phase progression speed, which remains unresolved.

The QBO is primarily a dynamic phenomenon driven by momentum forcing due to atmospheric waves (Lindzen and Holton, 1968; Holton and Lindzen, 1972). Observational and theoretical studies have demonstrated that a broad spectrum of atmospheric waves, generated by heat release from tropical convection, propagate vertically into the stratosphere (e.g., Holton, 1972; Salby and Garcia, 1987; Horinouchi and Yoden, 1996; Song et al., 2003; Song and Chun, 2005). They transport and deposit momentum to the flow in the stratosphere around the easterly/westerly jet of the QBO. This acts as the restoring force of the oscillation, advancing its phase (Lindzen and Holton, 1968; Holton and Lindzen, 1972). However, the flow in the tropical stratosphere is not purely horizontal but weakly upward on average (by less than $1\ \mathrm{mm\,s^{-1}}$) (Schoeberl et al., 2008; Kim and Chun, 2015b). Albeit very slow compared to horizontal motions, this upwelling advects substantial momentum, which can largely offset the wave forcing, thereby retarding the oscillation. Therefore, the theoretical hypothesis suggests that the fluctuation in the QBO progression speed could be explained by variations in the magnitude of upwelling and/or wave activity (e.g., Dunkerton, 1990; Kinnersley and Pawson, 1996; Hampson and Haynes, 2004; Kim et al., 2013; Krismer et al., 2013; Anstey et al., 2022a).

To date, no observational evidence has been found for the coherent variation of the wave activity with the fluctuating QBO periods (for a climate model result, see Krismer et al., 2013). A difficulty has existed in this issue because of the limitation of measurements in spatial resolution and coverage, given the ubiquitous convection over the tropics and the broad wave spectrum down to the $\sim$10 km scale in horizontal wavelength. On the other hand, the stratospheric upwelling is known to have a seasonal cycle (Mote et al., 1996, 1998; Schoeberl et al., 2008), and its possible effects on the QBO variability have been extensively studied using observational records and modeling approaches (e.g., Kinnersley and Pawson, 1996; Hampson and Haynes, 2004; Rajendran et al., 2018; Coy et al., 2020). In particular, it has been suggested that the seasonal dependence of QBO progression, including its stalling (Wallace et al., 1993; Kinnersley and Pawson, 1996), could result from the seasonal cycle of the upwelling.

Here, we use a global reanalysis data to investigate the fluctuations in the QBO period and progression speed. Our study reveals the underlying process driving these fluctuations, providing new evidence of the coherent variation of small-scale wave activity with the QBO periods.

2 Data and methods

2.1 Datasets

European Centre for Medium-Range Weather Forecasts (ECMWF) Reanalysis v5 (ERA5, Hersbach et al., 2020) data were used throughout the study. ERA5 is a global reanalysis spanning 1940 onward with a spatial resolution of $\sim$30 km. We used hourly wind and temperature data over the period of 1956–2015. The analysis period was determined to begin with the first observation of the QBO up to 10 hPa altitude. We excluded years after 2015 because the oscillation phases could not be unambiguously defined due to the QBO disruptions occurred in 2016 and 2019–2020 (e.g., Osprey et al., 2016). For the annual

https://doi.org/10.5194/egusphere-2024-3195
Preprint. Discussion started: 18 October 2024

cycle of precipitation, Long-Term Mean data from the Global Precipitation Climatology Project (GPCP) Monthly Analysis version 2.3 (Adler et al., 2003) were used.

2.2 QBO cycles and periods

Monthly and zonally averaged zonal winds over 5° N–5° S were used to describe the QBO. At each height, we defined an oscillation cycle as the period between the onsets of westerly winds. To avoid noise around zero wind and uniquely detect the onset of westerly winds, the 1-2-1 smoothing was applied three times to the monthly time series, but only when defining the cycle.

2.3 Wave momentum fluxes

Upward fluxes of eastward and westward momentum due to waves were calculated monthly, after decomposing them via Fourier transform in longitude and time. The eastward (westward) momentum fluxes were obtained by summing positive (negative) zonal-momentum fluxes in the Fourier domain where the zonal phase speeds were positive (negative). Absolute values were taken for the westward-momentum fluxes.

In this study, we refer to small-scale waves as those with zonal wavenumbers greater than 20 (wavelengths less than ~2000 km, i.e., gravity waves). When analyzing momentum fluxes of small-scale waves, only waves with zonal phase speeds greater than $\pm 5\ \mathrm{m\,s^{-1}}$ were considered. This phase speed threshold was applied to avoid noise in fluxes for small-scale waves with near-zero phase speeds.

2.4 Momentum forcing

The change rate of zonally averaged wind is expressed as

$$\frac{\partial \overline{u}}{\partial t} = \frac{\nabla \cdot \boldsymbol{F}}{\rho_0\, a \cos\phi} - \overline{w}^* \frac{\partial \overline{u}}{\partial z} + \overline{v}^* \hat{f} \tag{1}$$

by defining the Eliassen–Palm (EP) flux $\boldsymbol{F}$ and meridional and vertical velocities of the residual circulation $(\overline{v}^*, \overline{w}^*)$ following Andrews et al. (1987). Here, ρ_0, a, (ϕ, z) are the reference density, earth radius, and latitudinal and vertical coordinates, respectively; $\hat{f} := f - (a\cos\phi)^{-1}\partial(\overline{u}\cos\phi)/\partial\phi$, where f is the Coriolis parameter. The first two terms on the right-hand side of Eq. (1) represent the major components of momentum forcing in the equatorial stratosphere: wave forcing and vertical advection by upwelling, respectively. The terms in Eq. (1) were calculated using hourly data and averaged monthly. Additionally, an indirect estimate of the wave forcing was also obtained by subtracting all terms except the first on the right-hand side from the wind change rate in Eq. (1).

3 Characteristic behaviors of the QBO

Figure 1a shows the QBO of the tropical stratospheric wind with alternating phases, highlighting a large variation in its period (horizontal arrows) in the late 1990s–early 2000s (see Fig. 2 for the record of QBO periods since 1956). A characteristic

https://doi.org/10.5194/egusphere-2024-3195
Preprint. Discussion started: 18 October 2024

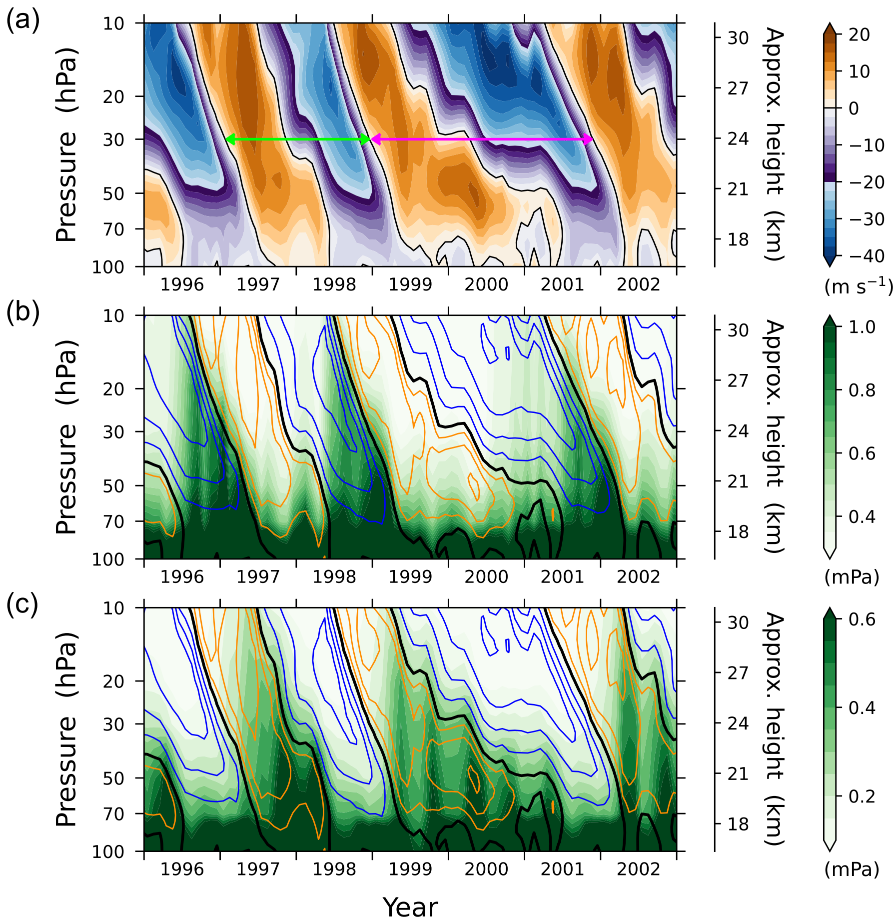

Figure 1. (a) Stratospheric zonal wind velocity averaged over 5° N–5° S. The green and magenta arrows indicate two examples of oscillation cycles at 30 hPa altitude, highlighting a large variation in the QBO period. (b, c) Upward fluxes of (b) eastward and (c) westward momentum due to atmospheric waves over 15° N–15° S (shading) along with the wind (yellow contours for westerlies at 5 $\mathrm{m\,s^{-1}}$ intervals; blue contours for easterlies at 10 $\mathrm{m\,s^{-1}}$ intervals; thick black contours for zero winds).

phenomenon associated with the period variation is the change in the descent speed of the easterly phase (Fig. 1a). The downward propagation of this phase often stagnates, as observed in the period from late 2000 through early 2001, resulting in a lengthening of the oscillation cycle. However, the downward speed of the westerly phase barely changes between cycles or within each cycle, as measured by the slopes of the zero-wind lines at the bounds of cycles in Fig. 1a. This results in the period of each cycle being nearly constant with height.

Another characteristic of the QBO is that the onset of westerly phases at 10 hPa coincides with the end of those phases at about 70 hPa (the bottom of the stratosphere), and the same pattern holds for easterly phases (Fig. 1a). This can be explained by the established theory of the interaction between atmospheric waves and flow (Holton and Lindzen, 1972; Plumb, 1977). Fig-

https://doi.org/10.5194/egusphere-2024-3195
Preprint. Discussion started: 18 October 2024

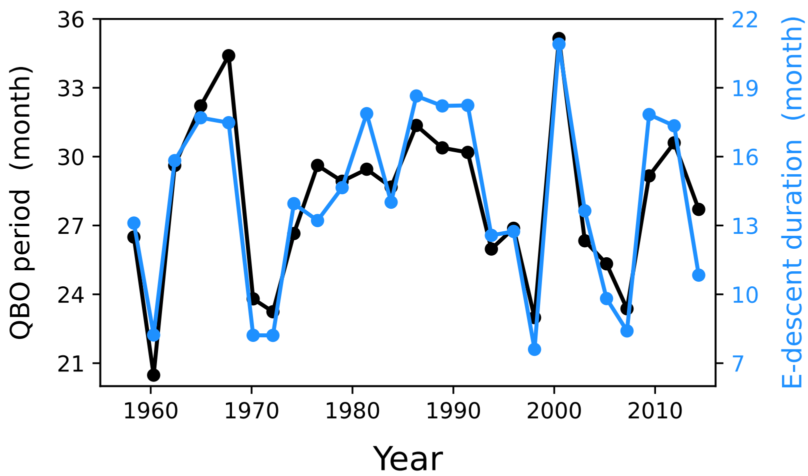

Figure 2. QBO period measured at 30 hPa (black), along with the duration of the easterly-phase descent from 15 hPa to 50 hPa (blue), for QBO cycles over 1956–2015. Pearson correlation of the two is 0.91.

ure 1b shows upward fluxes of eastward momentum carried by the waves. The eastward-momentum fluxes are largely reduced under the westerly flow condition, as the theory suggests. Therefore, at an arbitrary altitude, the fluxes can be substantial only when the flow is easterly throughout the layer below. The formation of such an easterly layer by the cease of the westerly phase at 70 hPa allows eastward momentum to be transported to $\sim$10 hPa altitude, acting as a conduit for the stream of momentum. The eastward momentum there forces the flow, leading to the transition to the westerly phase (Fig. 1b). Similarly, the westerly flow condition at the lower altitude works as a conduit for westward momentum (Fig. 1c), thereby controlling the onset of the easterly phase at $\sim$10 hPa.

Considering the aforementioned behaviors of the QBO, its period can also be estimated by the duration of westerly-phase descent through the layer from $\sim$10 hPa to 70 hPa plus that of easterly-phase descent. Furthermore, the variation of the period is predominantly caused by the latter, given that the descent speed of the westerly phase barely changes. To demonstrate this, the periods of the QBO from 1956 to 2015 are shown along with the durations of easterly-phase descent in Fig. 2. The phase descent was measured by tracking a constant zonal-wind velocity ($U_\varphi = -10\ \mathrm{m\,s^{-1}}$) within the easterly-shear layer between 15 hPa and 50 hPa. (This altitude range was chosen because the phase descent above 15 hPa was often too fast to measure using monthly data, while below 50 hPa, the descent was not clearly identifiable in some years due to the attenuation of the QBO near the tropopause.) Figure 2 demonstrates that variations in the duration of easterly-phase descent predominantly account for the variations in the period of whole cycle. The difference between the two is 14 months on average, with variations of less than ± 3 months. The results were not sensitive to the value of U_φ in the range of 0 to $-15\ \mathrm{m\,s^{-1}}$. Therefore, understanding the QBO period fluctuations primarily reduces to uncovering the process that controls the easterly-phase descent.

https://doi.org/10.5194/egusphere-2024-3195
Preprint. Discussion started: 18 October 2024

4 Variations in phase progression speed

4.1 Regression of phase descent speed

The descent speed of easterly phase, following a constant zonal-wind velocity U_φ in easterly shear, can be approximated as

$$-\dot{z}_\varphi = \frac{\partial \overline{u}}{\partial t}\left(\frac{\partial \overline{u}}{\partial z}\right)^{-1} \approx \rho_0^{-1}|\mathcal{F}(U_\varphi)| - \overline{w}^* \qquad (2)$$

from Eq. (1), while neglecting meridional gradient of wind near the equator. Here, $\mathcal{F}(c)$ denotes the spectral density of zonal-momentum flux with respect to the zonal phase speed of waves c, at the bottom of the stratosphere. Following Lindzen and Holton (1968), we consider the critical-level absorption to be the major wave-forcing mechanism, so that the EP flux divergence term in Eq. (1) has been approximated as $\rho_0^{-1}|\mathcal{F}(U_\varphi)|\,\partial\overline{u}/\partial z$.

Motivated by Eq. (2), we linearly regress the descent speed of the easterly phase at each pressure level (p) by

$$-\dot{z}_\varphi(p) \approx \alpha(p)F_{70} - \beta(p)W \qquad (3)$$

where F_{70} is the westward-momentum flux due to small-scale waves (see Sect. 2.3) averaged over 15° N–15° S at 70 hPa altitude, and W is the mass-weighted average of $\overline{w}^*$ ($\int \overline{w}^* \mathrm{d}p / \int \mathrm{d}p$) over the 10–70 hPa layer and over the same latitude band (representing the tropical stratospheric upwelling), with α and β being their regression coefficients. Here, the small-scale waves (with horizontal wavelengths less than ∼2000 km) are taken into account for F_{70}, as these have been inferred to be the primary source of the momentum forcing in the stratosphere during the descending easterly phase (e.g., Ern et al., 2014; Kim and Chun, 2015b). The wide latitude band was chosen to account for the lateral propagation of waves toward the equator (Kim et al., 2024). The spatial averaging applied to W aimed to reduce the effect of the QBO-induced local circulation on it (i.e., QBO-phase dependence). Since the regression was performed for a specific phase (with a given U_φ at p), it was unnecessary to include the phase dependence in independece variables.

Again, we used $U_\varphi = -10\ \mathrm{m\,s^{-1}}$ for the analysis, while the results were not sensitive to it in the range of 0 to $-15\ \mathrm{m\,s^{-1}}$. The regression was based on the monthly mean time series during 1956–2015, for the selected months when the QBO wind phase of U_φ appeared at around the target pressure p with the tolerance of $(1/8)p$. The numbers of samples were 124, 95, 107, 78, and 54, respectively, at 60, 50, 40, 30, and 20 hPa. These numbers correspond to 2–5 per QBO cycle on average. Note that the sampling at the monthly interval is appropriate, given that the small-scale wave momentum flux varies largely between months, as will be shown in Sect. 5. The selected time series of F_{70}, $-W$, and $-\dot{z}_\varphi$ were standardized prior to the regression to assess the relative contributions of the wave flux and stratospheric upwelling to the descent speed variation.

Figure 3a shows variations in the observed speed of the easterly-phase descent throughout 1956–2015 (the pressure scale height of 6.3 km was used here). The descent speed varies widely, as indicated by its standard deviation being comparable to its mean at each altitude, while it tends to increase with altitude. Figure 3b presents the standardized regression coefficients of F_{70} and $-W$ obtained for the descent speed at each altitude, along with the regression scores. A direct comparison between the observed and regressed speeds is shown in Fig. 4 for several altitudes (20, 30, 40, and 50 hPa). Overall, the regression scores are high (the regression correlations are 0.8–0.9 at most altitudes), with generally large coefficients of F_{70} (0.6–0.8) (Fig. 3b).

https://doi.org/10.5194/egusphere-2024-3195
Preprint. Discussion started: 18 October 2024

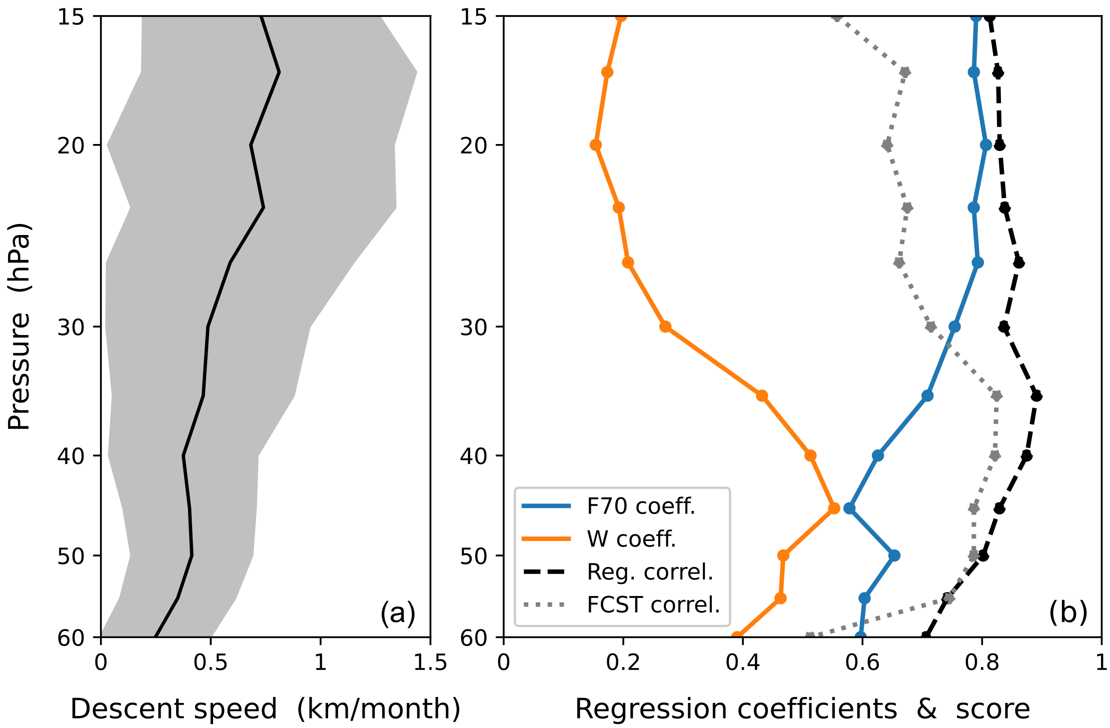

Figure 3. (a) Climatological mean (black line) and variation within one standard deviation (grey shading) of the descent speed of the easterly QBO phase (measured following the vertical trajectory of the $-10\ \mathrm{m\,s^{-1}}$ wind phase in easterly shear) throughout 1956–2015. (b) Standardized regression coefficients of 70 hPa small-scale westward-wave momentum flux (blue line) and stratospheric upwelling (orange line) for the descent speed at each altitude, along with the regression correlation score (black dashed line) (see the text for details of the regression). The grey dotted line in (b) depicts the correlation score of a hindcast using the obtained coefficients and the seasonal cycle of momentum flux and upwelling.

The coefficients of $-W$ are small at high altitudes ($\sim$0.2 at $p \lesssim 30$ hPa), but they increase at lower altitudes, reaching up to 0.55 at 45 hPa. The result indicates that the variation in the descent speed of the easterly phase depends primarily on the wave flux into the stratosphere, with the role of the upwelling variability being moderate or relatively minor except near 45 hPa.

Utilizing the obtained regression coefficients, a hindcast is performed using the climatological annual cycle of F_{70} and $-W$ as input. The correlation between the hindcasted and observed descent speeds (Fig. 3b, grey dotted line) is about 0.8 at 35–55 hPa, very close to the regression correlation there, and 0.65 at 17–25 hPa. This result indicates that the seasonal variation in wave flux and upwelling accounts for a large portion of the fluctuations in the descent speed of the easterly phase.

https://doi.org/10.5194/egusphere-2024-3195
Preprint. Discussion started: 18 October 2024

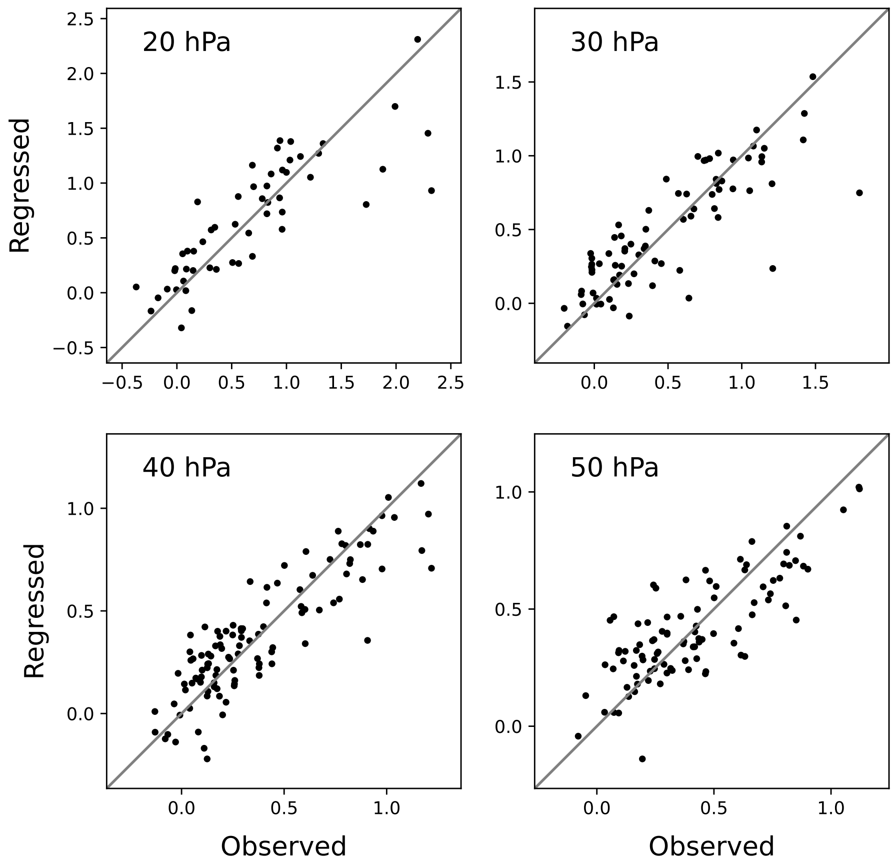

Figure 4. Scatter plots of observed versus regressed speeds of the easterly-phase descent (in km per month) at 20, 30, 40, and 50 hPa altitudes.

4.2 Temporal variations in momentum forcing

The time evolutions of wind and associated momentum forcing are analyzed at fixed altitudes to investigate the temporal variations of phase progression speed. Figure 5a and b show the time series of winds at 30 hPa (a middle level of the vertical QBO span) and their change rates, respectively, during the westerly-to-easterly transition phase in every QBO cycle in 1956–2015 (thin lines), as a function of calendar month. In all cycles, the phase progression occurs only during certain months: March to July and September to December, consistent with previous studies (e.g., Schenzinger et al., 2017). Accordingly, the cycles can be divided into three groups based on the pattern of phase progression. The first group (purple lines in Fig. 5) consists of cycles in which the phase change occurs essentially during March to July. The second group (green lines) includes cycles where the phase changes first to a weak easterly during September to December, stagnates until the following February, and then changes further in March to July. The third group (orange lines) experiences the first phase change in March to July and the final change in next March to July. (See Appendix A for the categorization procedure.) The thick lines in Fig. 5 represent

https://doi.org/10.5194/egusphere-2024-3195
Preprint. Discussion started: 18 October 2024

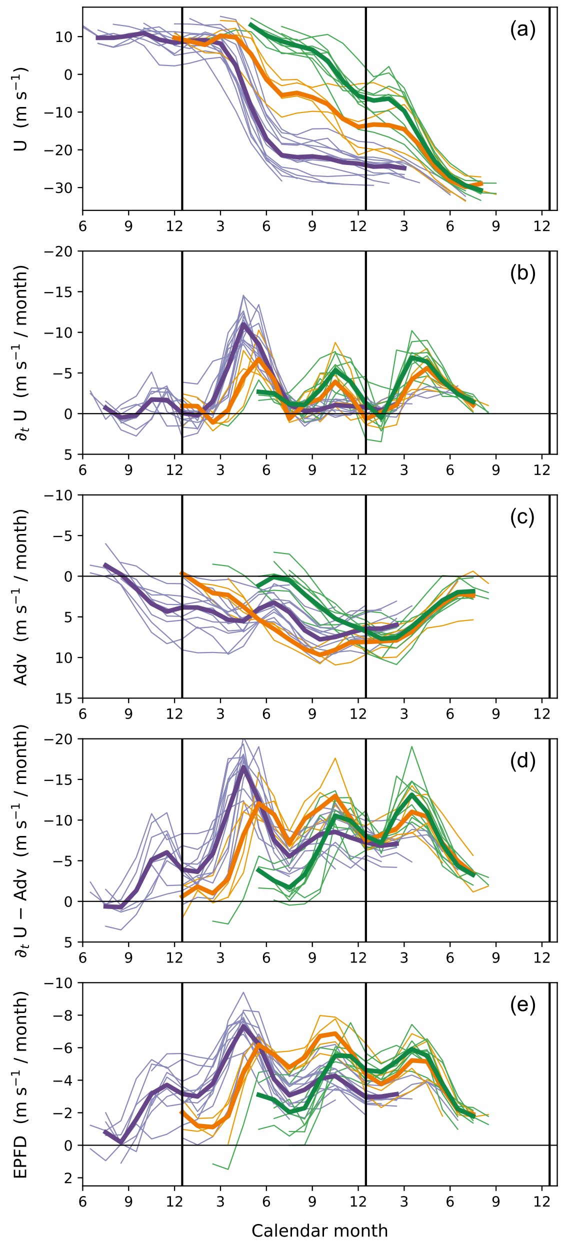

Figure 5. Time series at 30 hPa from the westerly-maximum to the easterly-maximum phase in each cycle of the QBO during 1956–2015 (thin lines), showing (a) the zonal wind over 5° N–5° S, (b) its tendency, (c) the sum of advection and Coriolis force (Adv), (d) the tendency with the contribution of Adv subtracted (i.e., (b) minus (c)), and (e) the Eliassen–Palm flux divergence, as a function of calendar month. The cycles are divided into three groups (indicated by different colors) based on the pattern of phase progression (see the text), and the averages for each group are plotted by thick lines.

https://doi.org/10.5194/egusphere-2024-3195
Preprint. Discussion started: 18 October 2024

the averaged time series for each group. Note that the stagnation of phase over time at a given altitude results in the stalling of phase descent (see Fig. 1a).

Figure 5c presents the contribution of meridional circulation ($\overline{v}^*, \overline{w}^*$) to the wind tendencies (i.e., sum of the vertical and meridional advection and the Coriolis force in Eq. (1)) at 30 hPa. In general, they have the opposite sign to the observed wind tendencies (cf. Fig. 5b), implying the retarding effect of the upwelling on the phase evolution. However, they show rather slow temporal variations that are not coherent with those of the observed tendencies, for each group of cycles. For quantitative comparison, Fig. 5d shows the portion of the wind tendencies with the contribution of meridional circulation subtracted (i.e., the tendencies minus all terms except the EP flux divergence in Eq. (1)). These time series still exhibit large monthly variations similar to the observed tendencies (Fig. 5b), with the two peaks in March to July and September to December, respectively. The result implies a relatively minor role of stratospheric upwelling in the temporal variability of QBO phase progression at 30 hPa, supporting the finding from Fig. 3b. Note that, given the momentum budget (Eq. (1)), the time series shown in Fig. 5d are regarded as an indirect estimate of the wave forcing, up to potential errors in upwelling velocity in the reanalysis data.

The direct estimate of the wave forcing, i.e., the explicitly calculated EP flux divergence, is presented in Fig. 5e. Its time series exhibit very similar temporal variations to the indirect estimate of the forcing (Fig. 5d) throughout the phase evolution: both estimates of the forcing start increasing in the early phase when the flow is westerly for each group (Fig. 5d, e, and a), and afterwards, they manifest the two peaks in annual variation. The forcing tends to weaken once the flow becomes strongly easterly. The temporal variations in the indirect estimate (Fig. 5d) suggest that the variability in wave forcing is the main driver of the observed (semi)annual behaviors of phase progression and stagnation at 30 hPa shown in Fig. 5a and b; this is ultimately confirmed by the agreement of the direct estimate of wave forcing (Fig. 5e). However, it should be noted that the magnitudes of the direct estimate are roughly half those of the indirect estimate (see the discussion in Sect. 6).

Qualitatively similar results are obtained at other altitudes as well. Figures 6 and 7 present the same analysis as Fig. 5 except at 20 hPa and 50 hPa, respectively. The westerly-to-easterly phase progression occurs during March to July and September to December but stagnates otherwise. This behavior is largely attributed to the wave forcing with its monthly variation. On the other hand, the semiannual variability in wind tendencies gets reduced as the altitude decreases, with slower phase progression during September to December than during March to July (panels b of Figs. 5–7).

The coherent variation of the wave forcing with the observed wind changes is striking, as this has never been revealed by previous reanalysis products or measurements. Existing reanalyses, except the one used here, have generally represented little wave forcing with indistinct monthly variations throughout the westerly-to-easterly transition phase of the QBO (see Appendix B for the results using two additional reanalysis datasets).

5 Seasonal modulation of wave activity

The monthly variation of the wave forcing shown in Fig. 5e is explained by the seasonal cycle of tropical convective activity and that of the wind in the tropopause layer, which both modulate the wave flux into the stratosphere. Figure 8a presents the climatological annual cycle of the upward flux of westward momentum due to the small-scale waves at 200 hPa ($\sim$12 km)

https://doi.org/10.5194/egusphere-2024-3195
Preprint. Discussion started: 18 October 2024

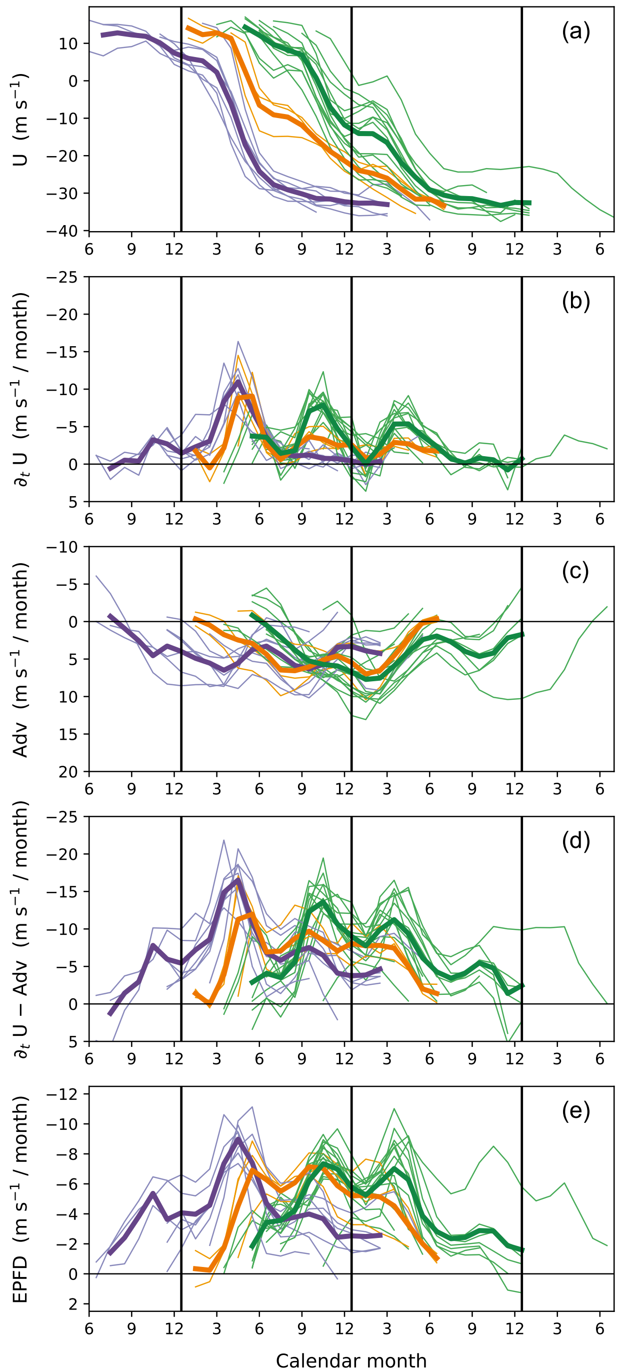

Figure 6. As in Fig. 5 except at 20 hPa.

https://doi.org/10.5194/egusphere-2024-3195
Preprint. Discussion started: 18 October 2024

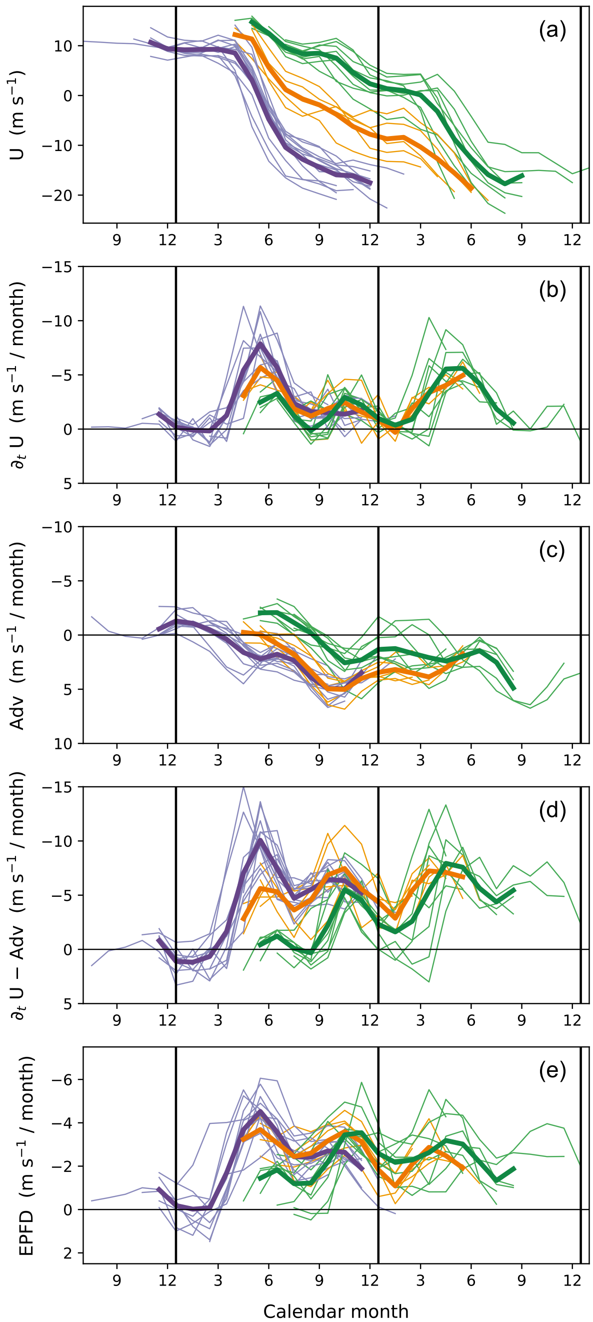

Figure 7. As in Fig. 5 except at 50 hPa. For better visibility, the time series are shown only after the wind at 30 hPa has transitioned to easterly.

https://doi.org/10.5194/egusphere-2024-3195
Preprint. Discussion started: 18 October 2024

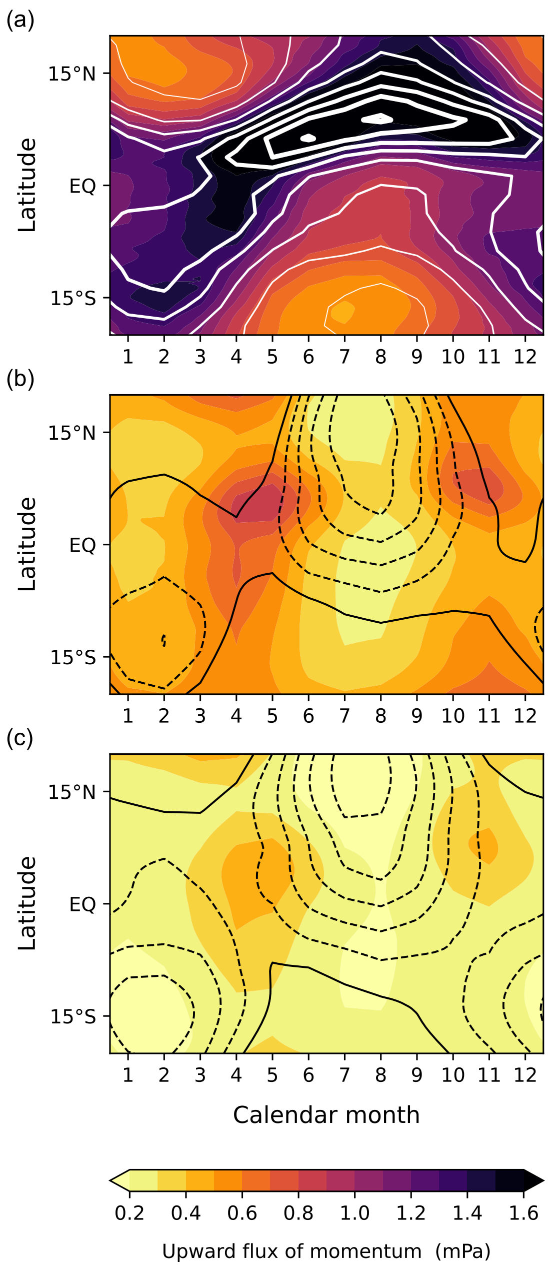

Figure 8. Climatological-mean annual cycle of upward flux of westward momentum due to waves with zonal wavelengths less than 2000 km (shading) at (a) 200 hPa, (b) 100 hPa, and (c) 70 hPa. The GPCP monthly precipitation rate is superimposed in (a) (white contours at intervals of $1\ \mathrm{mm\,d^{-1}}$). In (b) and (c), the vertical minima of zonal wind in the 100–200 hPa layer and the 70–200 hPa layer, respectively, are superimposed (black solid contours for zero winds; black dashed contours for easterlies at intervals of $3\ \mathrm{m\,s^{-1}}$).

https://doi.org/10.5194/egusphere-2024-3195
Preprint. Discussion started: 18 October 2024

altitude. In the upper troposphere, the spatio-temporal variation of the wave-momentum flux generally follows the seasonal cycle of precipitation (white contours in Fig. 8a), which is a proxy for convective activity as the source of waves.

However, the monthly variation of the flux is significantly altered in the tropopause layer, as shown at 100 hPa ($\sim$16 km) altitude (Fig. 8b). The 100 hPa flux exhibits two peaks, April–May and November, throughout the tropics, while the overall flux magnitude is reduced compared to that at 200 hPa. It is because of the dissipation of wave-momentum flux by the flow in the 200–100 hPa layer, which occurs more severely under the easterly condition for the flux of westward momentum due to gravity waves propagating westward. The flow in this layer (black contours in Fig. 8b) is easterly in the summer hemisphere. This condition, along with the weak convective activity in the winter hemisphere (Fig. 8a), results in relatively small fluxes during both solstices, with maxima occurring in April–May and November. A qualitatively similar monthly variation of the flux was previously obtained by Kim and Chun (2015a, Fig. 6) using a parameterization of convective gravity waves in a climate model, which supports the role of convection and tropopause-layer wind in the flux variation.

The flux at 70 hPa (Fig. 8c) shows a similar variation as that at 100 hPa with the same months of maxima, while being further dissipated in between. These months of maximum momentum flux into the stratosphere align with the peaks of wave forcing observed in the stratosphere (Fig. 5–7), explaining the monthly variation in the speed of QBO phase progression. This seasonal variation of the 70 hPa flux also explains a large portion of the fluctuations in the descent speed of easterly phase, as found in Fig. 3b (grey dotted line).

6 Summary and discussions

We revealed that the QBO period fluctuates primarily due to the temporal variation in the amount of westward momentum carried by small-scale waves (gravity waves). The speed of the easterly-phase descent, the key factor controlling the QBO period, was highly correlated with the gravity-wave momentum flux estimated in the tropical tropopause layer. Furthermore, the stratospheric momentum forcing exerted by the waves demonstrated coherent variations with the observed phase evolutions of the QBO. The annual variation of the wave-momentum flux was explained by the seasonal cycles of tropical convection and tropopause-layer wind. Other sources of variation, such as the El Niño–Southern Oscillation (ENSO) (Taguchi, 2010) and volcanic eruptions (DallaSanta et al., 2021), may also be involved on longer time scales. However, it is notable that the annual variation already accounts for the typical behaviors of phase progression and stagnation in observed QBO cycles. The contribution of stratospheric upwelling to the fluctuation of the QBO descent speed was found to be relatively minor above $\sim$40 hPa altitude but became comparable to the wave contribution below that level.

Although the primary target for atmospheric reanalysis products may have been to resolve synoptic-scale ($\sim$6000 km) weather systems and embedded larger-scale circulations, their resolutions are continuously improving beyond these scales. Our study demonstrates that waves with horizontal wavelengths less than $\sim$2000 km play a crucial role in QBO period fluctuations. It is encouraging that the reanalysis used here represents the interaction between these small-scale waves, convection, and the mean-flow oscillation with realistic variations, implying more opportunities for studies on multi-scale atmospheric phenomena beyond the synoptic scale. However, we also note that scales smaller than a few hundred kilometers are still largely truncated

https://doi.org/10.5194/egusphere-2024-3195
Preprint. Discussion started: 18 October 2024

in current-generation reanalyses, including the one used here. This limitation may have led to an underestimation of the wave flux and forcing presented in our results (cf. Fig. 5d and 5e), suggesting that the actual impact of small-scale waves could be even more significant than our analysis indicated.

Beyond the advancement in our understanding of QBO dynamics, these findings have important implications for both seasonal predictions and long-term climate projections. They suggest that prediction models should accurately represent the coupled variability of convection, small-scale waves, and the mean flow to improve seasonal forecasts of the QBO and related atmospheric teleconnections. This precise representation is also crucial for future climate projections of the QBO, which have shown a large spread between climate models (Butchart et al., 2020; Richter et al., 2022). By better capturing these multi-scale interactions, models may provide more reliable projections of future QBO behavior and its impacts on global climate.

Data availability. The ERA5 reanalysis data are publicly available at https://doi.org/10.24381/cds.143582cf. The GPCP monthly precipitation data can be obtained from the NOAA PSL website (https://psl.noaa.gov).

Appendix A: Procedure for QBO-cycle categorization

The categorization of cycles with respect to the pattern of westerly-to-easterly phase evolutions in Figs. 5–7 was motivated by their distinction into three groups as described in Sect. 4.2. For objective categorization, we used two criteria: the calendar month when the wind substantially weakened to less than U_1, and how the wind changed over the subsequent five months (U_2). With $U_1 = 0$ (except at 50 hPa where it was set to 5 $\mathrm{m\,s^{-1}}$), the QBO cycles in which the wind changed below U_1 in January to July were categorized into the first or second groups (purple and green lines, respectively, in Figs. 5–7); the other cycles were into the third group (orange lines). The first group was separated from the second by fast phase evolution with $U_2 < -20$, -15, and -8 $\mathrm{m\,s^{-1}}$ at 20, 30, and 50 hPa, respectively. The altitude dependence of U_1 and U_2 values was due to the vertical change in QBO amplitude.

Appendix B: Results from other reanalysis datasets

Two additional reanalysis products were used for comparison: ECMWF Interim Reanalysis (ERA-Interim, Dee et al., 2011) and Modern-Era Retrospective analysis for Research and Applications Version 2 (MERRA-2, Gelaro et al., 2017). ERA-Interim has a resolution of $\sim$80 km, spanning from 1979. MERRA-2 has a resolution of $\sim$50 km, from 1980.

Figures B1 and B2 show the evolutions of 30-hPa winds, tendencies, and momentum forcing during the westerly-to-easterly transition phase, as in Fig. 5, but using ERA-Interim and MERRA-2, respectively, during the period of 1980–2015. All the terms, except the EP flux divergence, exhibit qualitatively similar results with those using ERA5 (Fig. 5). However, the EP flux divergence obtained from these datasets is generally much smaller than that using ERA5, with indistinct temporal variations.

https://doi.org/10.5194/egusphere-2024-3195
Preprint. Discussion started: 18 October 2024

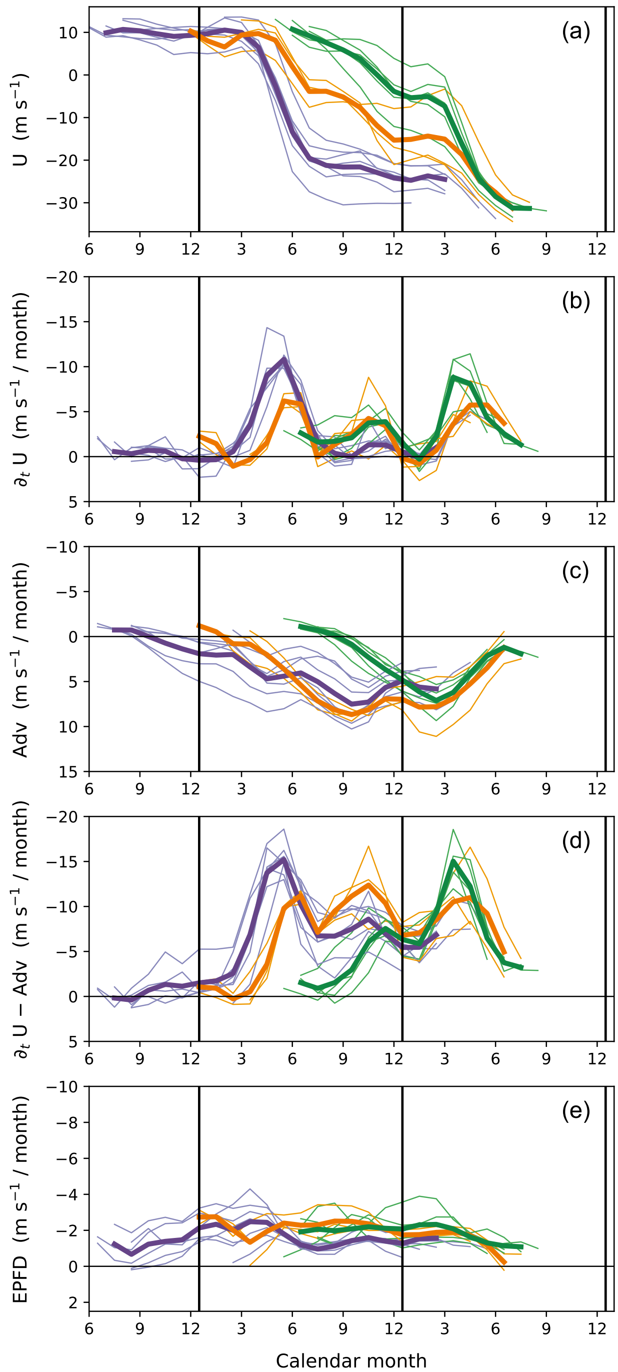

Figure B1. As in Fig. 5 except using ERA-Interim for the period of 1980–2015.

https://doi.org/10.5194/egusphere-2024-3195
Preprint. Discussion started: 18 October 2024

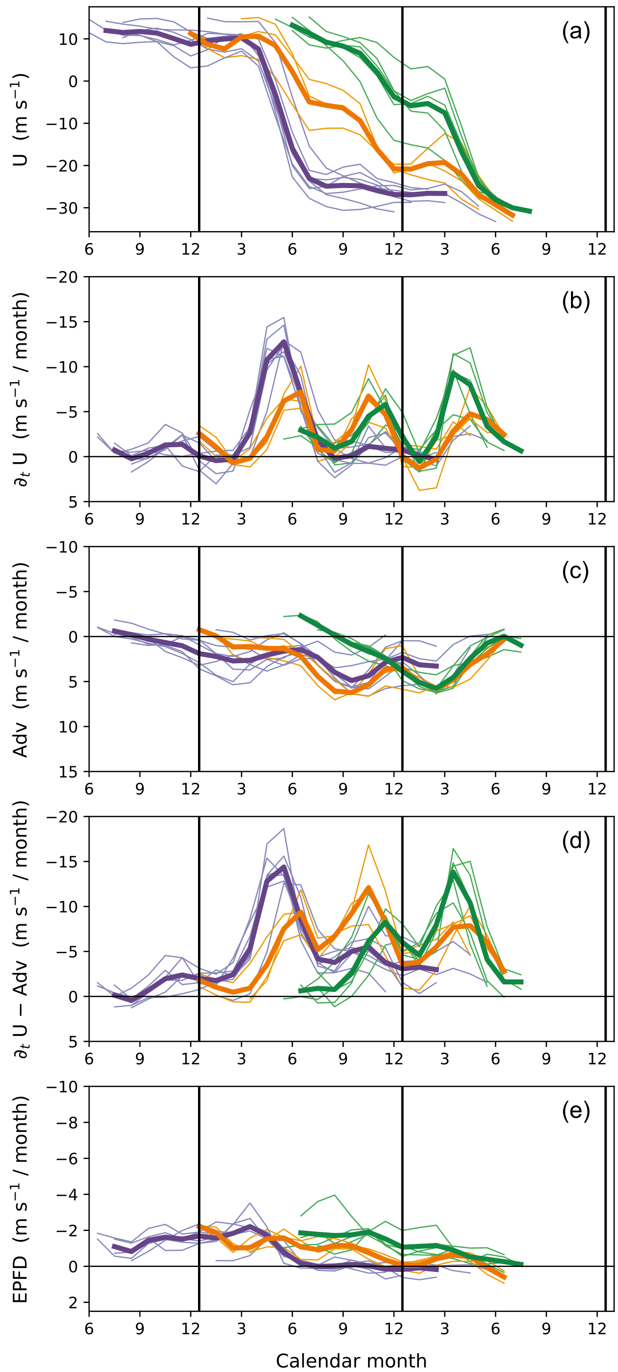

Figure B2. As in Fig. 5 except using MERRA-2 for the period of 1980–2015.

https://doi.org/10.5194/egusphere-2024-3195
Preprint. Discussion started: 18 October 2024

Author contributions. (This paper is single-authored.)

Competing interests. The author declares no competing interests.

Acknowledgements. This research was supported by Basic Science Research Program through the National Research Foundation of Korea (NRF) funded by the Ministry of Education (RS-2023-00244727), and also supported by the NRF grant funded by the Ministry of Science and ICT (RS-2024-00342219).

https://doi.org/10.5194/egusphere-2024-3195
Preprint. Discussion started: 18 October 2024

References

Adler, R. F., Huffman, G. J., Chang, A., Ferraro, R., Xie, P.-P., Janowiak, J., Rudolf, B., Schneider, U., Curtis, S., Bolvin, D., Gruber, A., Susskind, J., Arkin, P., and Nelkin, E.: The Version-2 Global Precipitation Climatology Project (GPCP) Monthly Precipitation Analysis (1979–Present), Journal of Hydrometeorology, 4, 1147–1167, https://doi.org/10.1175/1525-7541(2003)004<1147:TVGPCP>2.0.CO;2, 2003.

Andrews, D. G., Holton, J. R., and Leovy, C. B.: Middle Atmosphere Dynamics, Academic, 1987.

Anstey, J. A., Osprey, S. M., Alexander, J., Baldwin, M. P., Butchart, N., Gray, L., Kawatani, Y., Newman, P. A., and Richter, J. H.: Impacts, processes and projections of the quasi-biennial oscillation, Nature Reviews Earth & Environment, 3, 588–603, https://doi.org/10.1038/s43017-022-00323-7, 2022a.

Anstey, J. A., Simpson, I. R., Richter, J. H., Naoe, H., Taguchi, M., Serva, F., Gray, L. J., Butchart, N., Hamilton, K., Osprey, S., Bellprat, O., Braesicke, P., Bushell, A. C., Cagnazzo, C., Chen, C.-C., Chun, H.-Y., Garcia, R. R., Holt, L., Kawatani, Y., Kerzenmacher, T., Kim, Y.-H., Lott, F., McLandress, C., Scinocca, J., Stockdale, T. N., Versick, S., Watanabe, S., Yoshida, K., and Yukimoto, S.: Teleconnections of the Quasi-Biennial Oscillation in a multi-model ensemble of QBO-resolving models, Quarterly Journal of the Royal Meteorological Society, 148, 1568–1592, https://doi.org/10.1002/qj.4048, 2022b.

Baldwin, M. P., Gray, L. J., Dunkerton, T. J., Hamilton, K., Haynes, P. H., Randel, W. J., Holton, J. R., Alexander, M. J., Hirota, I., Horinouchi, T., Jones, D. B. A., Kinnersley, J. S., Marquardt, C., Sato, K., and Takahashi, M.: The quasi-biennial oscillation, Reviews of Geophysics, 39, 179–229, https://doi.org/10.1029/1999RG000073, 2001.

Bushell, A. C., Anstey, J. A., Butchart, N., Kawatani, Y., Osprey, S. M., Richter, J. H., Serva, F., Braesicke, P., Cagnazzo, C., Chen, C.-C., Chun, H.-Y., Garcia, R. R., Gray, L. J., Hamilton, K., Kerzenmacher, T., Kim, Y.-H., Lott, F., McLandress, C., Naoe, H., Scinocca, J., Smith, A. K., Stockdale, T. N., Versick, S., Watanabe, S., Yoshida, K., and Yukimoto, S.: Evaluation of the Quasi-Biennial Oscillation in global climate models for the SPARC QBO-initiative, Quarterly Journal of the Royal Meteorological Society, 148, 1459–1489, https://doi.org/10.1002/qj.3765, 2022.

Butchart, N., Anstey, J. A., Kawatani, Y., Osprey, S. M., Richter, J. H., and Wu, T.: QBO Changes in CMIP6 Climate Projections, Geophysical Research Letters, 47, e2019GL086 903, https://doi.org/10.1029/2019GL086903, 2020.

Coy, L., Newman, P. A., Strahan, S., and Pawson, S.: Seasonal Variation of the Quasi-Biennial Oscillation Descent, Journal of Geophysical Research, 125, e2020JD033 077, https://doi.org/10.1029/2020JD033077, 2020.

Coy, L., Newman, P. A., Molod, A., Pawson, S., Alexander, M. J., and Holt, L.: Seasonal Prediction of the Quasi-Biennial Oscillation, Journal of Geophysical Research: Atmospheres, 127, e2021JD036 124, https://doi.org/10.1029/2021JD036124, 2022.

DallaSanta, K., Orbe, C., Rind, D., Nazarenko, L., and Jonas, J.: Response of the Quasi-Biennial Oscillation to historical volcanic eruptions, Geophysical Research Letters, 48, e2021GL095 412, https://doi.org/10.1029/2021GL095412, 2021.

Dee, D. P., Uppala, S. M., Simmons, A. J., Berrisford, P., Poli, P., Kobayashi, S., Andrae, U., Balmaseda, M. A., Balsamo, G., Bauer, P., Bechtold, P., Beljaars, A. C. M., van de Berg, L., Bidlot, J., Bormann, N., Delsol, C., Dragani, R., Fuentes, M., Geer, A. J., Haimberger, L., Healy, S. B., Hersbach, H., Hólm, E. V., Isaksen, L., Kållberg, P., Köhler, M., Matricardi, M., McNally, A. P., Monge-Sanz, B. M., Morcrette, J.-J., Park, B.-K., Peubey, C., de Rosnay, P., Tavolato, C., Thépaut, J.-N., and Vitart, F.: The ERA-Interim reanalysis: configuration and performance of the data assimilation system, Quarterly Journal of the Royal Meteorological Society, 137, 553–597, https://doi.org/10.1002/qj.828, 2011.

https://doi.org/10.5194/egusphere-2024-3195
Preprint. Discussion started: 18 October 2024

Dunkerton, T. J.: Annual Variation of Deseasonalized Mean Flow Acceleration in the Equatorial Lower Stratosphere, Journal of the Meteorological Society of Japan. Ser. II, 68, 499–508, https://doi.org/10.2151/jmsj1965.68.4_499, 1990.

Ern, M., Ploeger, F., Preusse, P., Gille, J. C., Gray, L. J., Kalisch, S., Mlynczak, M. G., Russell, J. M., Riese, M., III, J. M. R., and Riese, M.: Interaction of gravity waves with the QBO: A satellite perspective, Journal of Geophysical Research, 119, 2329–2355, https://doi.org/10.1002/2013JD020731, 2014.

Flury, T., Wu, D. L., and Read, W. G.: Variability in the speed of the Brewer-Dobson circulation as observed by Aura/MLS, Atmospheric Chemistry and Physics, 13, 4563–4575, https://doi.org/10.5194/acp-13-4563-2013, 2013.

Garfinkel, C. I. and Hartmann, D. L.: The influence of the quasi-biennial oscillation on the troposphere in winter in a hierarchy of models. part II: Perpetual winter WACCM runs, Journal of the Atmospheric Sciences, 68, 2026–2041, https://doi.org/10.1175/2011JAS3702.1, 2011.

Gelaro, R., McCarty, W., Suárez, M. J., Todling, R., Molod, A., Takacs, L., Randles, C. A., Darmenov, A., Bosilovich, M. G., Reichle, R., Wargan, K., Coy, L., Cullather, R., Draper, C., Akella, S., Buchard, V., Conaty, A., da Silva, A. M., Gu, W., Kim, G.-K., Koster, R., Lucchesi, R., Merkova, D., Nielsen, J. E., Partyka, G., Pawson, S., Putman, W., Rienecker, M., Schubert, S. D., Sienkiewicz, M., and Zhao, B.: The Modern-Era Retrospective Analysis for Research and Applications, Version 2 (MERRA-2), Journal of Climate, 30, 5419–5454, https://doi.org/10.1175/JCLI-D-16-0758.1, 2017.

Gray, L. J., Anstey, J. A., Kawatani, Y., Lu, H., Osprey, S., and Schenzinger, V.: Surface impacts of the Quasi Biennial Oscillation, Atmospheric Chemistry and Physics, 18, 8227–8247, https://doi.org/10.5194/acp-18-8227-2018, 2018.

Hampson, J. and Haynes, P.: Phase alignment of the tropical stratospheric QBO in the annual cycle, Journal of the Atmospheric Sciences, 61, 2627–2637, http://journals.ametsoc.org/doi/pdf/10.1175/JAS3276.1, 2004.

Haynes, P., Hitchcock, P., Hitchman, M., Yoden, S., Hendon, H., Kiladis, G., Kodera, K., and Simpson, I.: The Influence of the Stratosphere on the Tropical Troposphere, Journal of the Meteorological Society of Japan. Ser. II, 99, 803–845, https://doi.org/10.2151/jmsj.2021-040, 2021.

Hersbach, H., Bell, B., Berrisford, P., Hirahara, S., Horányi, A., Muñoz-Sabater, J., Nicolas, J., Peubey, C., Radu, R., Schepers, D., Simmons, A., Soci, C., Abdalla, S., Abellan, X., Balsamo, G., Bechtold, P., Biavati, G., Bidlot, J., Bonavita, M., Chiara, G., Dahlgren, P., Dee, D., Diamantakis, M., Dragani, R., Flemming, J., Forbes, R., Fuentes, M., Geer, A., Haimberger, L., Healy, S., Hogan, R. J., Hólm, E., Janisková, M., Keeley, S., Laloyaux, P., Lopez, P., Lupu, C., Radnoti, G., Rosnay, P., Rozum, I., Vamborg, F., Villaume, S., and Thépaut, J.: The ERA5 global reanalysis, Quarterly Journal of the Royal Meteorological Society, 146, 1999–2049, https://doi.org/10.1002/qj.3803, 2020.

Holton, J. R.: Waves in the Equatorial Stratosphere Generated by Tropospheric Heat Sources, Journal of the Atmospheric Sciences, 29, 368–375, https://doi.org/10.1175/1520-0469(1972)029<0368:WITESG>2.0.CO;2, 1972.

Holton, J. R. and Lindzen, R. S.: An Updated Theory for the Quasi-Biennial Cycle of the Tropical Stratosphere, Journal of the Atmospheric Sciences, 29, 1076–1080, https://doi.org/10.1175/1520-0469(1972)029<1076:AUTFTQ>2.0.CO;2, 1972.

Holton, J. R. and Tan, H.-C.: The Influence of the Equatorial Quasi-Biennial Oscillation on the Global Circulation at 50 mb, Journal of the Atmospheric Sciences, 37, 2200–2208, https://doi.org/10.1175/1520-0469(1980)037<2200:tioteq>2.0.co;2, 1980.

Horinouchi, T. and Yoden, S.: Excitation of Transient Waves by Localized Episodic Heating in the Tropics and Their Propagation into the Middle Atmosphere, Journal of the Meteorological Society of Japan. Ser. II, 74, 189–210, https://doi.org/10.2151/jmsj1965.74.2_189, 1996.

https://doi.org/10.5194/egusphere-2024-3195
Preprint. Discussion started: 18 October 2024

Kim, Y.-H. and Chun, H.-Y.: Contributions of equatorial wave modes and parameterized gravity waves to the tropical QBO in HadGEM2, Journal of Geophysical Research, 120, 1065–1090, https://doi.org/10.1002/2014JD022174, 2015a.

Kim, Y.-H. and Chun, H.-Y.: Momentum forcing of the quasi-biennial oscillation by equatorial waves in recent reanalyses, Atmospheric Chemistry and Physics, 15, 6577–6587, https://doi.org/10.5194/acp-15-6577-2015, 2015b.

Kim, Y.-H., Bushell, A. C., Jackson, D. R., and Chun, H.-Y.: Impacts of introducing a convective gravity-wave parameterization upon the QBO in the Met Office Unified Model, Geophysical Research Letters, 40, 1873–1877, https://doi.org/10.1002/grl.50353, 2013.

Kim, Y.-H., Voelker, G. S., Bölöni, G., Zängl, G., and Achatz, U.: Crucial role of obliquely propagating gravity waves in the quasi-biennial oscillation dynamics, Atmospheric Chemistry and Physics, 24, 3297–3308, https://doi.org/10.5194/acp-24-3297-2024, 2024.

Kinnersley, J. S. and Pawson, S.: The Descent Rates of the Shear Zones of the Equatorial QBO, Journal of the Atmospheric Sciences, 53, 1937–1949, https://doi.org/10.1175/1520-0469(1996)053<1937:TDROTS>2.0.CO;2, 1996.

Kinnersley, J. S. and Tung, K. K.: Modeling the global interannual variability of ozone due to the equatorial QBO and to extratropical planetary wave variability, Journal of the Atmospheric Sciences, 55, 1417–1428, https://doi.org/10.1175/1520-0469(1998)055<1417:MTGIVO>2.0.CO;2, 1998.

Krismer, T. R., Giorgetta, M. A., and Esch, M.: Seasonal aspects of the quasi-biennial oscillation in the Max Planck Institute Earth System Model and ERA-40, Journal of Advances in Modeling Earth Systems, 5, 406–421, https://doi.org/10.1002/jame.20024, 2013.

Lindzen, R. S. and Holton, J. R.: A Theory of the Quasi-Biennial Oscillation, Journal of the Atmospheric Sciences, 25, 1095–1107, https://doi.org/10.1175/1520-0469(1968)025<1095:ATOTQB>2.0.CO;2, 1968.

Ling, X.-D. and London, J.: The Quasi-biennial Oscillation of Ozone in the Tropical Middle Stratosphere: A One-Dimensional Model, Journal of the Atmospheric Sciences, 43, 3122–3137, https://doi.org/10.1175/1520-0469(1986)043<3122:TQBOOO>2.0.CO;2, 1986.

Mote, P. W., Rosenlof, K. H., McIntyre, M. E., Carr, E. S., Gille, J. C., Holton, J. R., Kinnersley, J. S., Pumphrey, H. C., Russell, J. M., and Waters, J. W.: An atmospheric tape recorder: The imprint of tropical tropopause temperatures on stratospheric water vapor, Journal of Geophysical Research: Atmospheres, 101, 3989–4006, https://doi.org/10.1029/95JD03422, 1996.

Mote, P. W., Dunkerton, T. J., McIntyre, M. E., Ray, E. A., Haynes, P. H., and Russell, J. M.: Vertical velocity, vertical diffusion, and dilution by midlatitude air in the tropical lower stratosphere, Journal of Geophysical Research: Atmospheres, 103, 8651–8666, https://doi.org/10.1029/98JD00203, 1998.

Osprey, S. M., Butchart, N., Knight, J. R., Scaife, A. A., Hamilton, K., Anstey, J. A., Schenzinger, V., and Zhang, C.: An unexpected disruption of the atmospheric quasi-biennial oscillation, Science, 353, 1424–1427, https://doi.org/10.1126/science.aah4156, 2016.

Plumb, R. A.: The interaction of two internal waves with the mean flow: Implications for the theory of the quasi-biennial oscillation, Journal of the Atmospheric Sciences, 34, 1847–1858, https://doi.org/10.1175/1520-0469(1977)034<1847:TIOTIW>2.0.CO;2, 1977.

Rajendran, K., Moroz, I. M., Osprey, S. M., and Read, P. L.: Descent Rate Models of the Synchronization of the Quasi-Biennial Oscillation by the Annual Cycle in Tropical Upwelling, Journal of the Atmospheric Sciences, 75, 2281–2297, https://doi.org/10.1175/JAS-D-17-0267.1, 2018.

Randel, W. J. and Wu, F.: Isolation of the Ozone QBO in SAGE II Data by Singular-Value Decomposition, Journal of the Atmospheric Sciences, 53, 2546–2559, https://doi.org/10.1175/1520-0469(1996)053<2546:IOTOQI>2.0.CO;2, 1996.

Richter, J. H., Butchart, N., Kawatani, Y., Bushell, A. C., Holt, L., Serva, F., Anstey, J., Simpson, I. R., Osprey, S., Hamilton, K., Braesicke, P., Cagnazzo, C., Chen, C., Garcia, R. R., Gray, L. J., Kerzenmacher, T., Lott, F., McLandress, C., Naoe, H., Scinocca, J., Stockdale, T. N., Versick, S., Watanabe, S., Yoshida, K., and Yukimoto, S.: Response of the Quasi-Biennial Oscillation to a warming climate in global climate models, Quarterly Journal of the Royal Meteorological Society, 148, 1490–1518, https://doi.org/10.1002/qj.3749, 2022.

https://doi.org/10.5194/egusphere-2024-3195
Preprint. Discussion started: 18 October 2024

Salby, M. L. and Garcia, R. R.: Transient Response to Localized Episodic Heating in the Tropics. Part I: Excitation and Short-Time Near-Field Behavior, Journal of the Atmospheric Sciences, 44, 458–498, https://doi.org/10.1175/1520-0469(1987)044<0458:TRTLEH>2.0.CO;2, 1987.

Scaife, A. A., Athanassiadou, M., Andrews, M., Arribas, A., Baldwin, M., Dunstone, N., Knight, J., MacLachlan, C., Manzini, E., Müller, W. A., Pohlmann, H., Smith, D., Stockdale, T., and Williams, A.: Predictability of the quasi-biennial oscillation and its northern winter teleconnection on seasonal to decadal timescales, Geophysical Research Letters, 41, 1752–1758, https://doi.org/10.1002/2013GL059160, 2014.

Schenzinger, V., Osprey, S., Gray, L., and Butchart, N.: Defining metrics of the Quasi-Biennial Oscillation in global climate models, Geoscientific Model Development, 10, 2157–2168, https://doi.org/10.5194/gmd-10-2157-2017, 2017.

Schoeberl, M. R., Douglass, A. R., Stolarski, R. S., Pawson, S., Strahan, S. E., and Read, W.: Comparison of lower stratospheric tropical mean vertical velocities, Journal of Geophysical Research, 113, D24 109, https://doi.org/10.1029/2008JD010221, 2008.

Song, I.-S. and Chun, H.-Y.: Momentum Flux Spectrum of Convectively Forced Internal Gravity Waves and Its Application to Gravity Wave Drag Parameterization. Part I: Theory, Journal of the Atmospheric Sciences, 62, 107–124, https://doi.org/10.1175/JAS-3363.1, 2005.

Song, I.-S., Chun, H.-Y., and Lane, T. P.: Generation mechanisms of convectively forced internal gravity waves and their propagation to the stratosphere, Journal of the Atmospheric Sciences, 60, 1960–1980, https://doi.org/10.1175/1520-0469(2003)060<1960:GMOCFI>2.0.CO;2, 2003.

Stockdale, T. N., Kim, Y.-H., Anstey, J. A., Palmeiro, F. M., Butchart, N., Scaife, A. A., Andrews, M., Bushell, A. C., Dobrynin, M., Garcia-Serrano, J., Hamilton, K., Kawatani, Y., Lott, F., McLandress, C., Naoe, H., Osprey, S., Pohlmann, H., Scinocca, J., Watanabe, S., Yoshida, K., and Yukimoto, S.: Prediction of the quasi-biennial oscillation with a multi-model ensemble of QBO-resolving models, Quarterly Journal of the Royal Meteorological Society, 148, 1519–1540, https://doi.org/10.1002/qj.3919, 2022.

Taguchi, M.: Observed connection of the stratospheric quasi-biennial oscillation with El Niño–Southern Oscillation in radiosonde data, Journal of Geophysical Research, 115, 1–12, https://doi.org/10.1029/2010JD014325, 2010.

Thompson, D. W., Baldwin, M. P., and Wallace, J. M.: Stratospheric connection to Northern Hemisphere wintertime weather: Implications for prediction, Journal of Climate, 15, 1421–1428, https://doi.org/10.1175/1520-0442(2002)015<1421:SCTNHW>2.0.CO;2, 2002.

Wallace, J. M., Panetta, R. L., and Estberg, J.: Representation of the equatorial stratospheric quasi-biennial oscillation in EOF phase space, Journal of the Atmospheric Sciences, 50, 1751–1762, https://doi.org/10.1175/1520-0469(1993)050<1751:ROTESQ>2.0.CO;2, 1993.

Yoo, C. and Son, S.-W.: Modulation of the boreal wintertime Madden-Julian oscillation by the stratospheric quasi-biennial oscillation, Geophysical Research Letters, 43, 1392–1398, https://doi.org/10.1002/2016GL067762, 2016.